

# Performance Testing of Paper-based Electrochemical Sensor for Blood pH Measurements

Xingxing Cheng<sup>1</sup>, Changlong He<sup>1</sup>, Wei Zhang<sup>1</sup>, Huijin Wan<sup>1</sup>, Qiuna Shi<sup>1</sup> and Huilin Liu<sup>2,\*</sup>

<sup>1</sup> Outpatient Department, Qinhuangdao Jungong Hospital, Qinhuangdao, Hebei Province, 066001 China

<sup>2</sup> Cardiovascular Medicine Department (II), Qinhuangdao Jungong Hospital, Qinhuangdao, Hebei Province, 066001 China

\*E-mail: [hulin\\_drlu@163.com](mailto:hulin_drlu@163.com)

Received: 3 September 2022 / Accepted: 27 September 2022 / Published: 27 December 2022

---

A rapid pH test of blood is an important indicator to evaluate whether the blood has acidosis or alkalosis. Therefore, the rapid detection of blood pH is of great clinical importance. We propose a paper-based point-of-care (POC) electrochemical sensor for rapid pH detection in this work. Luteolin was used in the preparation of a dedicated detection electrode. The electrochemical oxidation peak of luteolin can be used as a probe to evaluate the pH conditions of the solution. In addition, we have systematically investigated uric acid in the blood that may impact detection accuracy. The results show that the presence of uric acid does not affect the detection performance of the sensor. Some other common ions also do not affect the results of the assay. Therefore, this proposed paper-based POC electrochemical sensor has the potential to detect pH in the blood rapidly.

---

**Keywords:** pH; Electrochemical sensor; Paper-based sensor; Uric acid; Luteolin

## 1. INTRODUCTION

The pH is the negative logarithm of the concentration of hydrogen ions in a solution and is a concise indicator of the concentration of H<sup>+</sup> in a solution [1,2]. The normal pH value in the blood is 7.35 to 7.45, determined by a combination of respiratory and metabolic factors. pH > 7.45 indicates the presence of alkalosis, while pH < 7.45 indicates the presence of acidosis. pH values in the normal range may indicate that the body's acid-base balance is maintained normally [3]. The pH of human blood does not exceed 7.35 to 7.45 due to the introduction of small amounts of acidic and alkaline substances because blood contains buffering substances [4]. When a small amount of acid (e.g., lactic acid, phosphoric acid) enters the blood, the pH of the blood does not decrease significantly because there is a large amount of HCO<sub>3</sub><sup>-</sup> in the blood, which can combine with the H<sup>+</sup> of the entering acid to form H<sub>2</sub>CO<sub>3</sub>

with a small degree of ionization, so that the concentration of hydrogen ions in the blood hardly increases [5]. When a small amount of base enters the blood, the  $H^+$  in the blood combines with the  $OH^-$  in the base to form  $H_2O$ , which is difficult to ionize. When the  $H^+$  in the blood decreases slightly, the  $H_2CO_3$  in the blood immediately ionizes  $H^+$  to replace the decreased  $H^+$  in the blood so that the pH of the blood does not increase significantly [6].

In parallel with the development of immunology and molecular biology, point-of-care (POC) technology has emerged. POC is designed to eliminate the need for complex sample pre-processing, allowing for on-the-spot sampling and immediate testing, and immediate test results [7,8]. So its two most prominent advantages are the speed of detection and the possibility of on-site analysis, which is impossible with other analytical methods. The outstanding advantage of the emerging paper-based sensors is that no additional method is required to transport the liquid; the device can use capillary action to transport the liquid to the measured region [9]. Emerging paper-based sensors do not require additional methods to transport the liquid and can use capillary action to transport the liquid to be measured to the area to be measured [10]. Paper-based sensors have the following advantages in the detection process: (1) minimal sample volume needs to be consumed; (2) paper-based devices can filter and separate components in the sample; (3) easy storage and transportation; and (4) used devices can be safely disposed of after simple incineration. Paper-based microchannels are often fabricated using printing techniques that can be mass-produced and can be made of hydrophobic materials such as paraffin or PDMS that are environmentally friendly and inexpensive [11]. In the future, paper-based sensors will provide a faster and cheaper method for bioassays that can detect multiple substances simultaneously [12]. Paper-based sensors combine the advantages of traditional paper tape testing with the practicality of sensors and have great potential for development in POC where instruments are not required. They are low cost, suitable for multiple analyte analysis, require small sample and reagent volumes, and are portable [13]. They are currently used to detect glucose, protein, lactate, uric acid, and cholesterol. The development of paper-based devices will drive the development of in situ instantaneous detection technology [14]. Using paper-based devices in combination with corresponding testing techniques can reduce the size of POC systems, reduce samples and reagents volume, and enable parallel detection of multiple analytes [15].

Paper-based platform can be further extended for more application after surface functionalization. The type of the paper for platform construction played a key role during the fabrication, where the Whatman No. 1 filter paper has been recommended as an excellent candidate [16]. Additionally, other paper such as waxed paper and glass fiber are also widely used. The main composition of the most commonly used cellulose paper is a homopolymer of (1→4)  $\beta$ -D-glucopyranose linked by acetal bonds and long chains of  $\beta$ -1,4-glucose with a polysaccharide structure [17,18]. Cellulose paper contains hydroxyl groups, which are negatively charged and can usually only adsorb cations and positively charged molecules [19]. However, the immobilization of biomolecules for modification requires a higher surface density of negative charges, and the modification of nanoparticles with negative surface charges on a paper base requires the use of cross-linking agents on the surface of the substrate or the addition of a surface coating [20].

Electrochemical analysis methods are characterized by low cost, simple operation, high selectivity, high sensitivity, simple instrumentation, and good portability, which are well suited for

building paper sensors [21]. The surface of paper can be easily used for electrode fabrication [23,24]. Cinti et al.[25] reported a paper-based screen-printed electrode biosensing device to detect ethanol in beer. The device was fabricated from ordinary office paper. It detects ethanol content in beer by detecting  $H_2O_2$  generated from the catalytic oxidation of ethanol by ethanol oxidase with a detection limit of 0.52 mM (0.003%, V/V). Electrochemical techniques can be used for the detection of nitrite in food [26]. Wang et al. [27] reported a disposable paper-based electrochemical sensor for sensitively detecting nitrite. Guadarrama-Fernández et al.[28] reported a novel paper-based sensor for glucose detection. This sensor was used to rapidly detect glucose in orange juice by potentiometric detection with a sensitivity of  $-119.6 \pm 6.4$  mV/dec, a detection range of 0.03-1.0 mM, and a detection limit of 0.02 mM. We propose a new, simple, and extremely low-cost paper-based electrochemical sensor in this work. The paper-based electrochemical sensor consists of a paper-based sensor and a three-electrode system. The three electrodes are fixed on the paper-based channel by molten paraffin, and the analytical solution reaches the reaction area of the paper-based channel due to capillary action. This paper-based POC detection technique was used for pH detection in blood.

## 2. EXPERIMENTS

### 2.1. Fabrication of paper-based electrochemical sensor

All chemicals used in this work were analytical grade and used without further purification. The fabrication process of paper-based sensors is shown in Figure 1. First, two PDMS microchannel pattern masters are stacked together and completely cover the middle layer of filter paper. The PDMS pattern master with the filter paper sandwiched is fixed by double-sided adhesive tape. Then, the pattern master sandwiched with a filter paper is dipped into the preheated molten paraffin wax and placed in a thermostat (temperature set to  $75^\circ\text{C}$ ) for about 2s. The paper-based sensors can be obtained by taking out and waiting for the wax to solidify naturally and finally peeling off the master mask. The width of the paper-based sensor is 4 mm, and the length is 10 mm. The thickness of Whatman 1 Chr cellulose filter paper is 0.18 mm.

The POC sensor uses a three-electrode system, with the auxiliary and reference electrodes being gold electrodes. The working electrode is a specially designed sensing electrode. Mix 0.10 g of lignocaine with 1.0 g of graphite powder and mix well. In a flat bottom glass cylinder, add 3.0 mL of tetrahydrofuran and 0.400 g of PVC powder and stir to dissolve the PVC completely. Add the aforementioned mixture and stir thoroughly to form a suspension. Then add 30  $\mu\text{L}$  of dibutyl phthalate and let the tetrahydrofuran evaporate completely to obtain the electrode film. The membrane is cut into strips, the wire is inserted at one end, and then the wire end is embedded with 10 mm of molten solid paraffin to obtain a working electrode.

Integration of electrochemical microelectrodes based on already fabricated paper-based sensors. Three electrodes of 0.1 mm diameter were placed on the paper-based microfluidic channel at 1 mm equal spacing, followed by fixing the electrodes outside the channel with molten paraffin and keeping the electrodes inside the channel tightly attached to the paper-based channel. A layer of molten paraffin is applied to the hydrophobic area of the paper-based channel, and then the paper-based channel of the

same size and shape is covered. The double paper-based channels are tightly fitted together, and three electrodes can be fixed in the middle of the double paper-based channels.

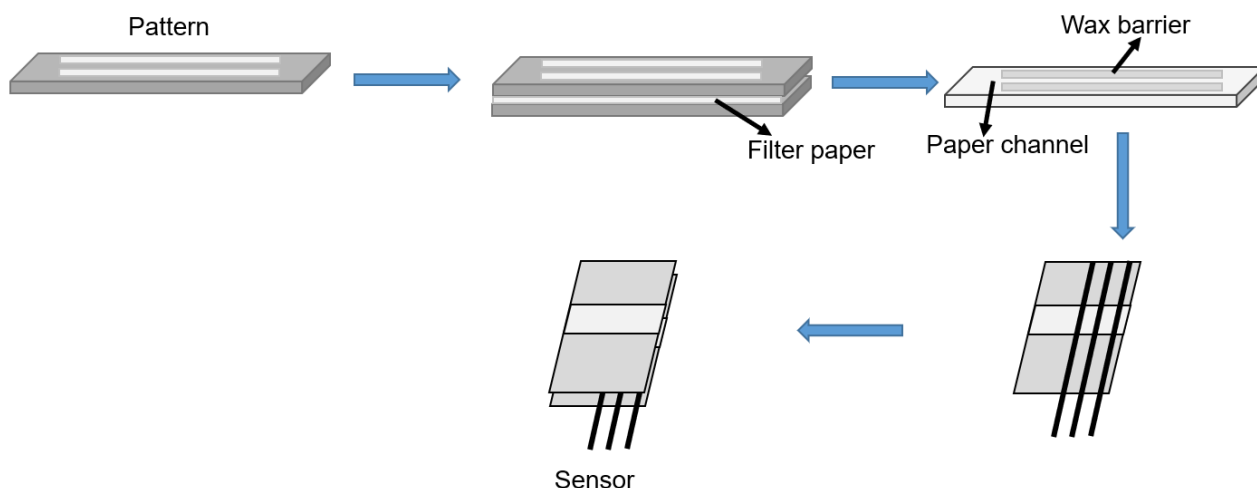


**Figure 1.** Fabrication process of paper-based POC electrochemical sensor.

## 2.2. Electrochemical measurements

**POC sensor performance testing:** Electrochemical experiments were conducted at room temperature using cyclic voltammetry with a CHI760E electrochemical workstation with an initial potential of 0.3V and a termination potential of -0.1 V. A mixture of 2 mM ferrocenecarboxylic acid and 0.5 M potassium chloride was dropped onto the entrance of the paper-based channel. Cyclic voltammograms were recorded at different scan rates.

**pH test:** The oxidation peak potential  $E_{pa}$  (square wave increment of 0.01 V, square wave amplitude of 0.05 V, square wave frequency of 20 Hz) was recorded in the range of -0.6 to 1.3 V, with -0.6 V as the starting potential.

**Uric acid test:** Wait for 200 s at a starting potential of 0 V in the voltage range of 0 to 1.0 V, then perform a square wave scan (potential increment of 0.01 V, square wave amplitude of 0.1 V, square wave frequency of 20 Hz) and record the oxidation peak current.

## 3. RESULTS AND DISCUSSION

The cyclic voltammograms (CV) of 2 mM ferrocenecarboxylic acid solution at different scan rates are shown in Figure 2. The scan rates in Figure 2 are 50, 100, 200, 300, 400, 500 mV/s. The CV of 2 mM ferrocenecarboxylic acid solution of the sensor is a typical reversible electrochemical reaction. The difference between the reduction peak ( $E_{pc}$ ) and the oxidation peak ( $E_{pa}$ ) within the scan rate of 50-500 mV/s is about 0.067 V, which is very close to the theoretical value of 0.059 V [31]. Where the scan rate ranges from 200-500 mV/s, the peak anode current is linearly proportional to the square root of the scan rate. The peak current ratio ( $i_{pa}/i_{pc}$ ) is approximately equal to 1. This reversible reaction indicates that no interference reaction occurs [32].

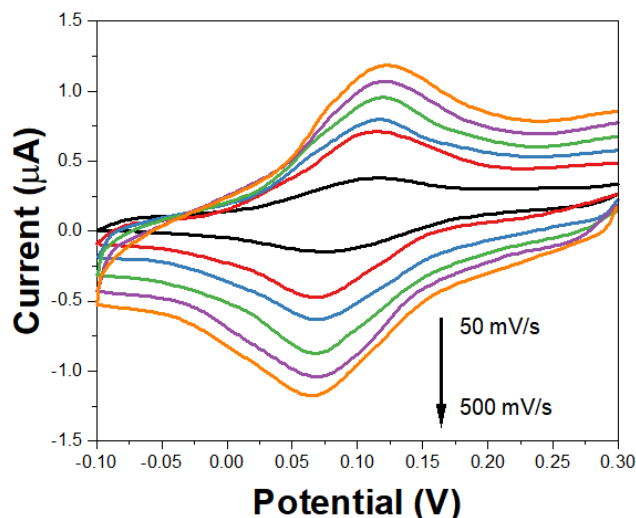


**Figure 2.** CV of POC paper-based electrochemical sensor towards 2 mM ferrocene.

PBS in the pH range of 2.00~8.00 was applied dropwise to the surface of the POC paper-based electrochemical sensor, and the square wave voltammetric curves (SWV) were recorded. As shown in Figure 3A, an oxidation peak appears on all curves, attributed to luteolin in the working electrode, and its peak potential shifts negatively with increasing pH. This negative shift showed a good linear relationship with pH conditions (Figure 3B). The linear regression equation was  $E_{pa}(V) = -0.0541 \text{ pH} + 0.642$  ( $r = 0.998$ ), based on which the pH determination could be performed.

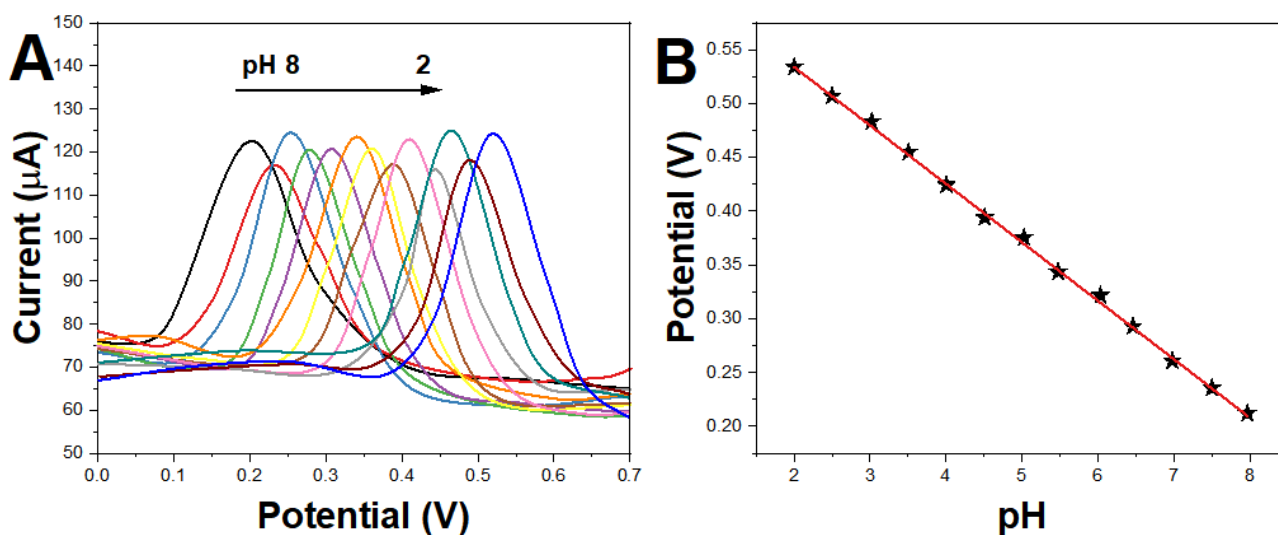


**Figure 3.** (A) Square wave voltammetry curves of POC paper-based electrochemical sensor at different pH value and (B) oxidation peak potential vs pH value.

The effect of uric acid in blood on the test results needs to be considered because it is electrochemically active and has a relatively similar oxidation potential to that of luteolin [33]. We

investigated the SWV response of uric acid at different concentrations in PBS at pH 7.4. Uric acid showed an oxidation peak and the peak current increased with increasing concentration (Figure 4). The detection limit was  $1.88 \times 10^{-7}$  M.

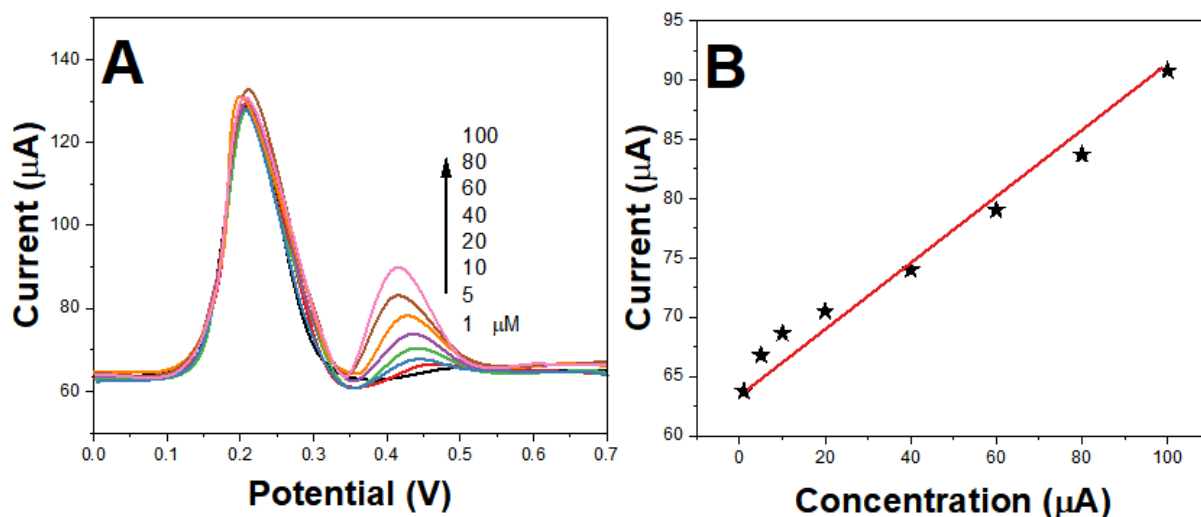


**Figure 4.** (A) Square wave voltammetry curves of POC paper-based electrochemical sensor at different concentrations of uric acid and (B) oxidation peak potential vs concentrations of uric acid.

The peak current of electrochemical oxidation of uric acid is related to the pH value of the medium. This study investigated the peak currents of 70 and 90 μM uric acid at different pH values. At pH 3.50 to 5.00, the peak current increased with increasing pH [34]. At pH 5.00 to 8.00, the peak current decreased with increasing pH (Figure 5). The peak currents of uric acid showed a linear relationship with pH in the ranges of pH 3.50 to 5.00 and pH 5.00 to 8.00, respectively. The relationship between pH and *i<sub>pa</sub>* and the linear equation slope showed that the peak currents varied with pH in the same way in both groups.

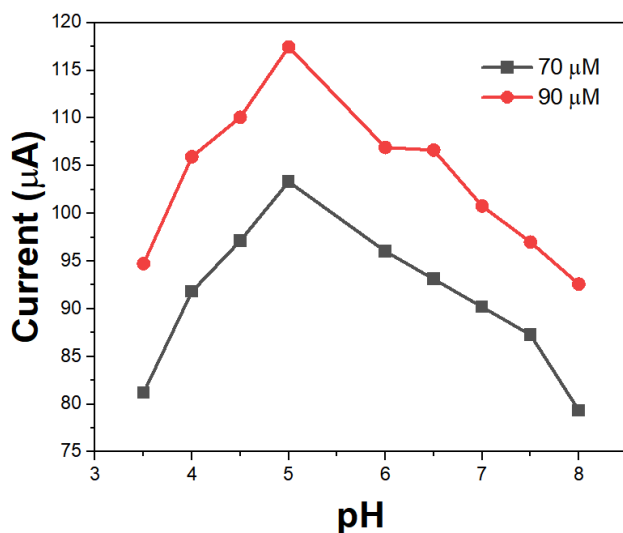


**Figure 5.** Effect of pH value on peak current of 70 and 90 μM uric acid.

Five sets of POC paper-based electrochemical sensors were prepared by the same method to detect PBS at pH 7.0. The results were 7.34, 7.31, 7.31, 7.29 and 7.32 with RSDs of 0.3%, indicating that the reproducibility of this electrode was good. The peak potentials of the commercially available standard buffer solutions at pH 4.00 and pH 6.86 were measured five times in parallel for each solution, and the experimental results are shown in Table 1.

**Table 1.** pH determination results of pH buffer solution using fabricated POC paper-based electrochemical sensor.

Sample	Results	Relative error (%)	RSD
pH 4.0 buffer	3.85	-3.3	0.3
pH 6.86 buffer	6.84	2.2	0.4
Blood 1	7.43	1.4	0.3
Blood 2	7.42	1.2	0.3

We then investigated the interference of  $Mg^{2+}$ ,  $Ca^{2+}$ ,  $Al^{3+}$ ,  $FeCl_3$ ,  $KNO_3$ , and uric acid as coexisting components in the pH determination. Solutions containing  $1.0 \times 10^{-3}$  M of the above components were prepared in PBS at pH 7.40, and  $E_{pa}$  was measured and pH was calculated according to the experimental method (Figure 6A). The relative errors of the results ranged from 0.6% to 4.6% (Figure 6B), indicating that none of the above components interfered with the determination of pH value under the premise of allowing  $\pm 5\%$  relative error.

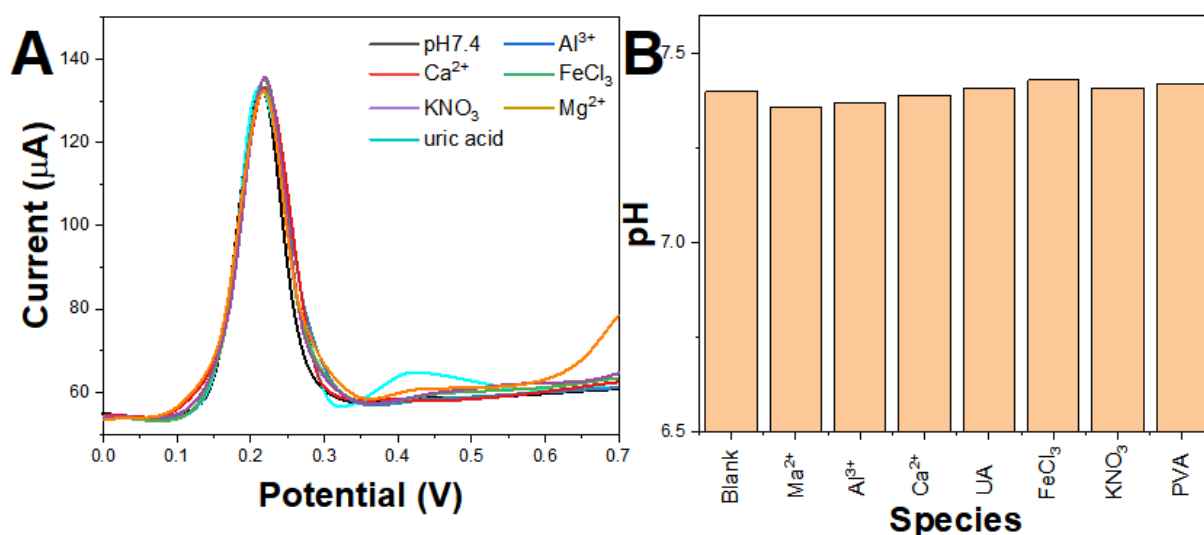


**Figure 6.** (A) Square wave voltammetry curves of POC paper-based electrochemical sensor in pH 7.4 with co-existence of  $Mg^{2+}$ ,  $Ca^{2+}$ ,  $Al^{3+}$ ,  $FeCl_3$ ,  $KNO_3$  and UA. (B) Relative error of coexisting components on determination results of pH.

Blood contains traces of fatty acids, enzymes, proteins, and other macromolecules, so the pH value was determined at 0.1% neutral surface. Therefore, the effect of 0.1% neutral surfactant polyvinyl alcohol (PVA) as a coexisting model was investigated on the pH determination [35]. The results showed that the peak current and peak potential were almost unchanged during pH determination and did not interfere with the results.

#### 4. CONCLUSIONS

We prepared a new paper-based POC electrochemical sensor and validated the device's electrochemical performance using 2 mM ferrocenecarboxylic acid solution. A method for pH determination of human blood was established using this POC sensor. This assay technique can be used for rapid clinical blood analysis. Luteolin was immobilized into the working electrode for the pH probe. The oxidation peak can accurately know the pH of the solution of lignocaine. In addition, the effect of uric acid in blood was systematically investigated. The results indicate that the proposed paper-based POC electrochemical sensor is a very promising strategy for pH detection of blood.

#### References

1. M. Baghayeri, S. Nabavi, E. Hasheminejad, V. Ebrahimi, *Topics in Catalysis*, 65 (2022) 623–632.
2. B. Jørgenrud, E. Skadberg, J. de Carvalho Ponce, H. Furuhaugen, T. Berg, *Journal of Pharmacological and Toxicological Methods*, 107 (2021) 106939.
3. K. Kirsch, J. Detilleux, D. Serteyn, C. Sandersen, *PLoS One*, 14 (2019) e0211104.
4. P. Mengarda, F.A.L. Dias, J.V.C. Peixoto, R. Osiecki, M.F. Bergamini, L.H. Marcolino-Junior, *Sensors and Actuators B: Chemical*, 296 (2019) 126663.
5. D. Uner-Bahar, I. Isildak, *Int. J. Electrochem. Sci.*, 15 (2020) 12724–12739.
6. O. Özbek, Ö. Isildak, I. Isildak, *Biochemical Engineering Journal*, 176 (2021) 108181.
7. C.-K. Choi, S.M. Shaban, B.-S. Moon, D.-G. Pyun, D.-H. Kim, *Analytica Chimica Acta*, 1170 (2021) 338630.
8. M. de L. Gonçalves, L.A. Truta, M.G.F. Sales, F.T. Moreira, *Analytical Letters*, 54 (2021) 2611–2623.
9. K. Kirsch, J. Detilleux, D. Serteyn, C. Sandersen, *PLoS One*, 14 (2019) e0211104.
10. S. Lin, X. Hu, J. Lin, S. Wang, J. Xu, F. Cai, J. Lin, *Analyst*, 146 (2021) 4391–4399.
11. G. Jiang, W. Su, C. Zhang, W. Deng, X. Wang, Z. Yang, X. Lv, C. Lu, S. Li, R. Ma, X. Huang, L. Ye, M. Wang, W. Yu, *Ecological Indicators*, 142 (2022) 109302.
12. J.J. Manoranjitham, S.S. Narayanan, *Food Chemistry*, 342 (2021) 128246.
13. H. Yu, Z. Tong, T. Bai, Z. Mao, X. Ni, J. Ling, *Journal of Applied Polymer Science*, 138 (2021) 50802.
14. Z. Zhao, Z. Zhao, B. Fu, J. Wang, W. Tang, *Journal of Soils and Sediments*, 21 (2021) 689–697.
15. C. Hohmann, R. Pfister, K. Kuhr, J. Merkle, J. Hinzmann, G. Michels, *Critical Care Research and Practice*, 2019 (2019) 9838706.
16. T. Beduk, E. Bihar, S.G. Surya, A.N. Castillo, S. Inal, K.N. Salama, *Sensors and Actuators B: Chemical*, 306 (2020) 127539.
17. D. Harpaz, E. Eltzov, T. Axelrod, R.S. Marks, A.I.Y. Tok, *Biochemical Engineering Journal*, 155 (2020) 107483.



18. K. Hiraka, K. Kojima, W. Tsugawa, R. Asano, K. Ikebukuro, K. Sode, *Biosensors and Bioelectronics*, 151 (2020) 111974.
19. X.-X. Li, D. Tian, C.-H. He, J.-H. He, *Electrochimica Acta*, 296 (2019) 491–493.
20. C.M. Moreira, M.L. Scala-Benuzzi, E.A. Takara, S.V. Pereira, M. Regiart, G.J.A.A. Soler-Illia, J. Raba, G.A. Messina, *Talanta*, 200 (2019) 186–192.
21. S. Xu, X. Li, G. Sui, R. Du, Q. Zhang, Q. Fu, *Chemical Engineering Journal*, 381 (2020) 122666.
22. F. Arduini, S. Cinti, V. Caratelli, L. Amendola, G. Palleschi, D. Moscone, *Biosensors and Bioelectronics*, 126 (2019) 346–354.
23. V.N. Ataide, L.F. Mendes, L.I. Gama, W.R. de Araujo, T.R. Paixão, *Analytical Methods*, 12 (2020) 1030–1054.
24. C.C. de Souza, G.F. Alves, T.P. Lisboa, M.A.C. Matos, R.C. Matos, *Journal of Food Composition and Analysis*, 112 (2022) 104700.
25. S. Cinti, M. Basso, D. Moscone, F. Arduini, *Analytica Chimica Acta*, 960 (2017) 123–130.
26. K.S. Prasad, X. Cao, N. Gao, Q. Jin, S.T. Sanjay, G. Henao-Pabon, X. Li, *Sensors and Actuators B: Chemical*, 305 (2020) 127516.
27. P. Wang, M. Wang, F. Zhou, G. Yang, L. Qu, X. Miao, *Electrochemistry Communications*, 81 (2017) 74–78.
28. L. Guadarrama-Fernández, M. Novell, P. Blondeau, F.J. Andrade, *Food Chemistry*, 265 (2018) 64–69.
29. M. Amatongchai, J. Sitanurak, W. Sroysee, S. Sodanat, S. Chairam, P. Jarujamrus, D. Nacapricha, P.A. Lieberzeit, *Analytica Chimica Acta*, 1077 (2019) 255–265.
30. F. Ma, X. Li, Y. Li, Y. Feng, B.-C. Ye, *Talanta*, 250 (2022) 123756.
31. G.V. Martins, A.C. Marques, E. Fortunato, M.G.F. Sales, *Electrochimica Acta*, 284 (2018) 60–68.
32. C. Srisomwat, P. Teengam, N. Chuaypen, P. Tangkijvanich, T. Vilaivan, O. Chailapakul, *Sensors and Actuators B: Chemical*, 316 (2020) 128077.
33. P.J. Lamas-Ardisana, G. Martínez-Paredes, L. Añorga, H.J. Grande, *Biosensors and Bioelectronics*, 109 (2018) 8–12.
34. T. Pholsiri, A. Lomae, K. Pungjunun, S. Vimolmangkang, W. Siangproh, O. Chailapakul, *Sensors and Actuators B: Chemical*, 355 (2022) 131353.
35. Q. Cao, B. Liang, T. Tu, J. Wei, L. Fang, X. Ye, *RSC Advances*, 9 (2019) 5674–5681